ACS APPLIED MATERIALS & INTERFACES

Research Article

www.acsami.org

One-Dimensional Au–ZnO Heteronanostructures for Ultraviolet Light Detectors by a Two-Step Dielectrophoretic Assembly Method

Haitao Ding, Jinyou Shao,* Yucheng Ding, Weiyu Liu, Hongmiao Tian, and Xiangming Li

Micro- and Nano-manufacturing Research Center, State Key Laboratory for Manufacturing Systems Engineering, Xi'an Jiaotong University, Xi'an, Shaanxi 710049, China

ABSTRACT: One-dimensional ZnO decorated with metal nanoparticles has received much attention in the field of ultraviolet light detection because of its high photosensitivity and fast response, while how to form effective metal–ZnO heterostructures cost efficiently is still in development. We report an efficient and well-controlled method to form Au–ZnO heterostructures by two-step dielectrophoretic assembly. First, ZnO nanowires dispersed in deionized water were assembled dielectrophoretically in a planar microelectrode system. To control the number and position of assembled ZnO nanowires, a planar triangle-shaped microelectrode pair was imposed with a high-frequency ac voltage signal in this assembly process. Then a droplet of Au nanoparticle suspension was applied to decorate the preformed ZnO nanowire by another dielectrophoretic assembly process. The near-field dielectrophoretic force induced by the existence of ZnO nanowire spanning the electrode gap attracts Au nanoparticles onto the surface of ZnO nanowires and forms effective Au–ZnO heterostructures. After the adsorption of Au nanoparticles, the performances of Au–ZnO heteronanostructures in UV detection were studied. Experimental results indicate that the ratio of the photo-to-dark current of the Au–ZnO heteronanostucture-based detector was improved significantly, and the photoresponse was accelerated considerably. This kind of enhancement in performance can be attributed to the localized Schottky junctions on the surface of ZnO nanowire which improves the surface band bending.

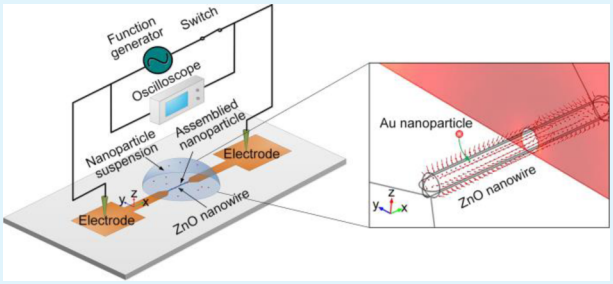

KEYWORDS: *ZnO nanowire, ultraviolet photodetector, dielectrophoretic assembly, Au nanoparticle*

1. INTRODUCTION

Ultraviolet (UV) detection has attracted considerable interest for a wide range of applications in chemical and environmental monitoring, optical communications, and our daily life.[1] ZnO nanowire is a promising semiconductor nanomaterial with a wide band gap of 3.34 eV, large exciton binding energy of 60 meV, stable chemical properties, and high electrochemical activity, making it appropriate for fabricating devices such as sensors[2−8] and actuators,[9−11] especially in UV light detection.[12,13] In the past few years, studies on a one-dimensional ZnO nanostructure-based UV light detector mainly focused on improving the photoresponse performance using ZnO nanowires decorated with metal nanoparticles. Because a Schottky junction is formed between a metal nanoparticle and a ZnO nanowire, a charge depletion region is created around the nanoparticle. Thus, compared with a bare ZnO nanowire-based device, the photocurrent and sensitivity of the hybrid nanostructure can be enhanced. Sputtering and surface deposition of a metal layer have been used to fabricate the metal–ZnO heterostrutures.[14−16] However, as the nanoparticles begin to accumulate, metal nanoparticle chains bridging the microelectrode pair can be formed, for the microelectrodes and the substrate are also decorated with the metal when ZnO nanowires are modified. The electric current passes through the nanoparticle chains instead of the ZnO nanowires. Schottky junctions cannot be created between the metal nanoparticles and the ZnO nanowires, thus decreasing the performance of the device. Electrospinning has produced Ag–ZnO heterostructures for UV detection,[17,18] but along with the photocurrent and response speed of the device being improved, it has resulted in a remarkable increase of dark current. The nanoparticle–nanowire hybrid structure can also be chemically synthesized using organic ligands as the linkers,[19,20] but they brought contaminations to the pure system of the particles and nanowires. Therefore, it is very important to develop an efficient method for the metal nanoparticle–ZnO nanowire-based device that can control the number and position of nanoparticles on the surface of the ZnO nanowires, maximize the performance of the device, and maintain the pure system of the nanoparticles and nanowires at one time.

Dielectrophoresis (DEP) has been proved to be a convenient way to manipulate and assemble nanomaterials onto the designated positions precisely.[21−28] This paper reports an efficient and well-controlled two-step method for fabricating the Au–ZnO heterostructures by the DEP force. First, a single

Received: February 11, 2015
Accepted: May 26, 2015
Published: May 26, 2015

DOI: 10.1021/acsami.5b01362
ACS Appl. Mater. Interfaces 2015, 7, 12713−12718

ZnO nanowire dispersed in deionized water (DI) was assembled dielectrophoretically in a planar microelectrode system. Also, the ZnO nanowire—a channel bridging the microelectrode pair—can be formed. Then, after an electrical voltage is applied to the microelectrodes, a droplet of Au nanoparticle suspension is dripped into the microelectrode system with a ZnO nanowire channel. The DEP force induced by the electric field in the solution attracts Au nanoparticles onto the surface of ZnO nanowires. Moreover, the effects of metal nanoparticles on the surface of ZnO nanowires on UV-light-detection performance were investigated. The photoresponse and response speed of the ZnO nanowire-based UV light detector were significantly enhanced by the DEP adsorption of metal nanoparticles on the surface of ZnO nanowires.

2. EXPERIMENTAL DETAILS

In this study, a microelectrode system was fabricated by an electron-beam lithography and lift-off process. In particular, a thin film of ZEP520 (positive electron resist, Zeon Co.) was spin casted on an insulating SiO_2 substrate. To improve its conductivity, a 10 nm Al thin film was deposited on the resist by the magnetron sputtering method. After electron beam exposure, the sample was immersed in a NaOH solution to remove the Al layer and developed in ZED-N50 (developer of ZEP520, Zeon Co.). A 10 nm Cr layer for adhesion enhancement and a 70 nm Pd layer were successively deposited on the prepatterned resist. Finally, the metal layer on the resist was removed using *N,N*-dimethylacetamide, affording the final microelectrode structure on an insulating SiO_2 surface.

A powder of ZnO nanowires with a 200 nm diameter and 4−5 μm length was used, commercially available from Sigma-Aldrich. The powder of ZnO nanowires was dispersed in DI water and sonicated for 30 min. A droplet of the ZnO nanowire suspension (0.05%, w/v) was dripped over the microelectrode system, and then a sinusoidal voltage signal with an amplitude of 3 V and frequency of 10−600 kHz was applied to the microelectrode pair by a function generator (Agilent 33220A) using needle probes (Wentworth Laboratories, MP1008). After 120 s, the ZnO droplet was removed with a slow stream of nitrogen. Figure 1a shows the size and geometric configuration of the microelectrode system with a ZnO nanowire, and the nearest distance between the electrodes is 3 μm.

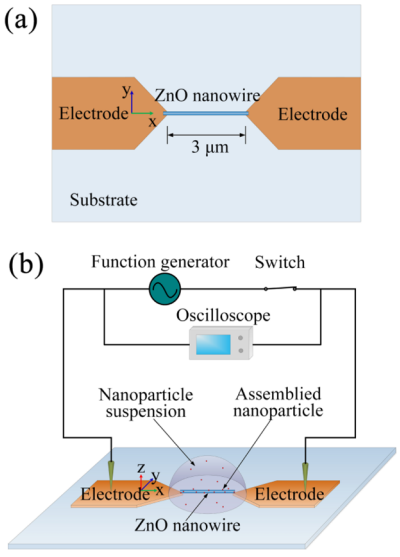

Figure 1. (a) Size configuration of a ZnO nanowire-based microelectrode system. (b) Experimental setup used in the DEP assembly of Au nanoparticles.

The DEP assembly of a gold nanoparticle (20 nm in diameter) suspension from BBI (British Biocell International) was performed with a voltage signal of 3 V amplitude and from 500 kHz to 1 MHz frequency on the microelectrode system for 60 s. Figure 1b shows the experimental setup of the microelectrode system. Finally, the generator was switched off, and the sample was washed in DI water and dried with a slow stream of nitrogen.

3. RESULTS AND DISCUSSION

3.1. Single ZnO Nanowire Manipulation Dieletrophoretically. There is considerable interest in manipulating nanowires, such as ZnO nanowire, by DEP assembly, which is a convenient methodology to manipulate them onto the designated positions precisely. Recent studies have reported on the technique with a high alignment yield for single nanowires from statistical data in multiple electrode pairs.[29−31] In our experiment, we studied the behaviors of ZnO nanowires in a separate microelectrode pair and not in multiple electrode pairs, which is the prerequisite and foundation for the performance study of a single-ZnO-nanowire-based device. The reproducibility experiments in a separate microelectrode pair carried out show that the obtained test results are similar and reliable. Although the photocurrent of a device based on ZnO nanowires in parallel is higher than on a single ZnO nanowire, the photosensitivity decreases significantly with the increase in the number of ZnO nanowires.[32] Hence, the photodetector in our experiment is based on a single ZnO nanowire in a separate microelectrode pair.

For a better understanding of the DEP assembly of ZnO nanowires, numerical calculation of the electric field distribution was conducted using the finite element method. The electric field in sinusoidal steady state obeys charge conservation derived using time harmonic analysis[33]

$$\nabla\cdot\tilde{\boldsymbol{J}} = \nabla\cdot[(\sigma + j\omega\varepsilon)\cdot(-\nabla\tilde{V})] = 0 \quad (1)$$

Here, $\tilde{\mathbf{J}}$ is the complex electric current density and $\tilde{V}$ the potential phasor. $\omega = 2\pi f$ is the angular frequency of the applied voltage signal. ε and σ are the dielectric permittivity and electric conductivity of the corresponding computational domain ($\varepsilon = 80\varepsilon_0$, $\varepsilon_0 = 8.85 \times 10^{-12}$ F/S is the vacuum permittivity, $\sigma = 10^{-5}$ S/m). In this case, eq 1 can be simplified into Laplace's equation $\nabla\tilde{V} = 0$.

Figure 2a shows the electric field distribution of a triangle-shaped electrode system at 3 V. As the voltage is maintained, the electric field distribution remains identical for different frequency. The maximum field intensity is reached in the immediate vicinity of the electrode tip. Because the DEP force acting on a single ZnO nanowire increases with the gradient of squared field intensity at a frequency,[34] it is also strongest at the electrode tip where numerous ZnO nanowires can be adsorbed dieletrophoretically.

Figure 2b−d shows SEM photographs of the DEP-assembled ZnO nanowires at various frequencies. With increasing frequency, the number of DEP-assembled ZnO nanowires decreases apparently under the same DEP assembly time. At 600 kHz, a single ZnO nanowire was captured between the microelectrode pair, which indicates the ac frequency employed exerts an influence on the DEP assembly behavior of ZnO nanowires. In fact, the DEP force decreases with increasing frequency, resulting in a decline in the number of adsorptions of nanowires. In the following, this paper investigated the DEP assembly of Au nanoparticles in the ZnO-nanowire-based microelectrodes.

DOI: 10.1021/acsami.5b01362
ACS Appl. Mater. Interfaces 2015, 7, 12713−12718

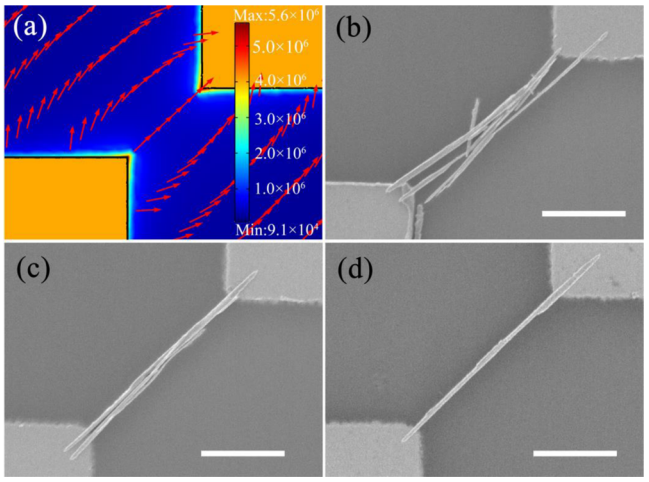

Figure 2. (a) Electric field distribution of a triangle-shaped electrode system at 3 V (units V/m). SEM photographs of the DEP-assembled ZnO nanowires at various frequencies: (b) 10 (c) 100, and (d) 600 kHz. Scale bars are 1 μm.

3.2. DEP-Assembly of Au Nanoparticles in a ZnO-Nanowire-Based Microsystem. To elucidate the mechanism of the Au nanoparticle motion, numerical modeling was performed based on the theory of particle DEP around ZnO nanowires. At frequencies of hundreds of kilohertz, Maxwell–Wagner interfacial charge relaxation dominates the structural polarization between two materials of different electrical properties, and the DEP force acting on these interfacial dielectric gradients would transport more polarizable medium to occupy the regions of higher field intensity.[35] For the spherical nanoparticles subjected to a background electric field, the net DEP force can be expressed by the point–dipole approximation as follows[33]

$$\langle \mathbf{F}_{\mathbf{DEP}} \rangle = \pi \varepsilon_f R^3 \mathrm{Re}[f_{CM}(\omega)] \nabla(\tilde{\mathbf{E}} \cdot \tilde{\mathbf{E}}^*) \quad (2)$$

The frequency dependence of the DEP force consists of the Clausius–Mossotti (CM) factor as follows

$$f_{\mathrm{CM}}(\omega) = \frac{\tilde{\varepsilon}_\mathrm{p} - \tilde{\varepsilon}_\mathrm{f}}{\tilde{\varepsilon}_\mathrm{p} + 2\tilde{\varepsilon}_\mathrm{f}} \quad (3)$$

where R is the equivalent radius of the spherical nanoparticles, Re(...) is the real part operator, $\tilde{\mathbf{E}}$ is the phasor amplitude of the field vector, i.e., $\boldsymbol{E}(t)$ = Re($\tilde{\boldsymbol{E}}e^{j\omega t}$), and $\tilde{\boldsymbol{E}}^*$ is the complex conjugate part. The subscripts p and f represent the particle and fluid, respectively. $\tilde{\varepsilon}_{\mathrm{p,f}} = \varepsilon_{\mathrm{p,f}} - j\frac{\sigma_{\mathrm{p,f}}}{\omega}$ is the complex permittivity of a lossy dielectric, and ε and σ are the real dielectric constant and conductivity, respectively. In this paper, $\varepsilon_\mathrm{p} = 1.6\varepsilon_0$ and $\varepsilon_\mathrm{f} = 80\varepsilon_0$ (ε_0 = 8.85 × 10−12 F/S is the vacuum permittivity), σ_p = 0.02 S/m and $\sigma_\mathrm{f} = 10^{-5}$ S/m.

Figure 3a shows the real component of the CM factor for the used 20 nm particle. When Re$[f_{\mathrm{CM}}(\omega)] > 0$, the nanoparticles are more polarizable than the surrounding liquid; thus, a positive DEP (p-DEP) force will push them along the field gradients toward stronger field areas. Otherwise, when Re$[f_{\mathrm{CM}}(\omega)] < 0$, they are subjected to a n-DEP force that repels them away from the high-field regions. The inset of Figure 3a shows that a computational domain of the cubic shape for potential distribution with confined but enough space (200 × 160 × 100 μm^3) is considered. Two cross-sections representing the DEP force were selected to characterize the motion of the nanoparticles.

The DEP force reaches its maximum value at both ends of the nanowire compared with the rest of the ZnO nanowire (Figure 3b), and the direction vector of p-DEP force points to the surface of the ZnO nanowires where the electric field intensity is strong (Figure 3c), indicating that it attracts nanoparticles to the vicinity. Figure 3d shows that the forces applied on the nanoparticles in the vicinity of the ZnO

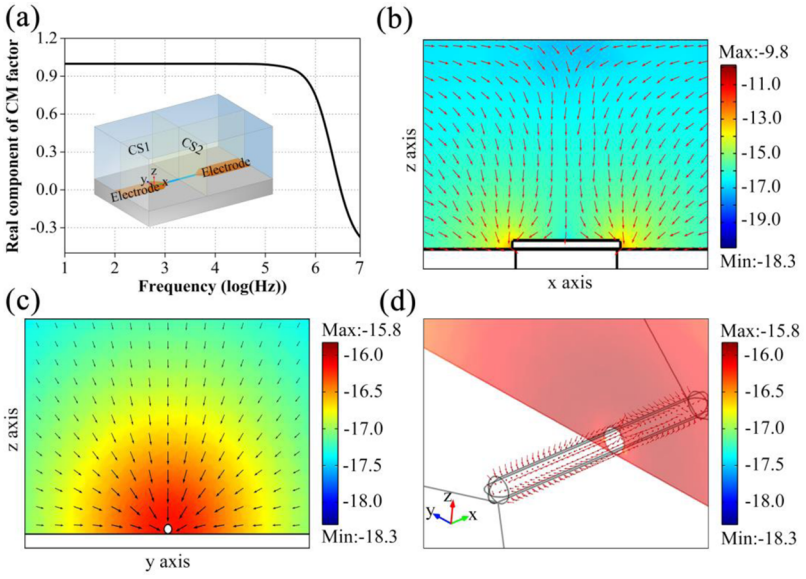

Figure 3. Illustration of DEP assembly of Au nanoparticles in a ZnO-nanowire-based microsystem. (a) Real part of the CM factor of the 20 nm Au nanoparticle with respect to its suspending medium as a function of driving frequency. (Inset) Computational domain of the electric field. Cross-section 1 (CS1) indicates the symmetrical x–z cross section, and cross-section 2 (CS2) denotes the y–z cross section in the assembly region. Spatial distribution of particle DEP force at 500 kHz around a ZnO nanowire between the electrodes: (b) in CS1, (c) in CS2, and (d) in the vicinity of the surface of the ZnO nanowire (color plotted on the log scale, units 10^x N).

DOI: 10.1021/acsami.5b01362
ACS Appl. Mater. Interfaces 2015, 7, 12713–12718

nanowire point to the surface of the wire. Therefore, the nanoparticles could be assembled onto the surface of the ZnO nanowires. With increasing assembly time, much more nanoparticles aggregated on the surface of ZnO nanowires because of a stronger field intensity in the region and patterned into a nanoparticle layer to wrap up the ZnO nanowire. During the nanoparticle assembly, the ZnO nanowires acted as effective channels that adsorbed the metal nanoparticles and oriented the growth of the nanoparticle layer.

The SEM photographs in Figure 4a and 4c show the DEP assembly of a ZnO nanowire between the microelectrode pair at a frequency of 600 kHz and a voltage of 3 V amplitude. A single ZnO nanowire assembled to form a channel, connecting the electrode pair. After the DEP assembly of Au nanoparticles at 3 V and 1 MHz, the ZnO nanowire has been decorated with the nanoparticles (Figure 4b). Much more nanoparticles settled down on the surface of the ZnO nanowires in the vicinity of the tips of the electrodes than the rest. When the frequency of the electrical signal decreased to 500 kHz, numerous Au nanoparticles aggregated on the surface of the ZnO nanowires and covered the entire surface (Figure 4d).

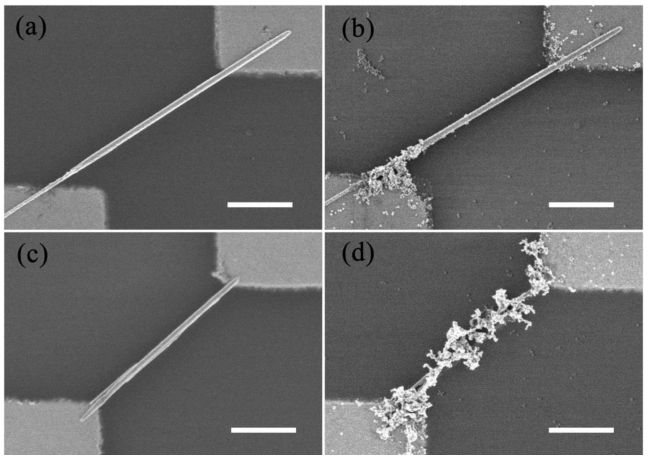

Figure 4. SEM photographs of the DEP-assembled ZnO nanowires decorated at 1 MHz without (a) and with (b) Au nanoparticles and at 500 kHz without (c) and with (d) Au nanoparticles. Scale bars are 1 μm.

3.3. UV Detection of the Devices. The photoresponse behaviors of the devices without and with Au nanoparticles (the experimental results of Figure 4c and 4d) were studied at room temperature. Figure 5a shows the $I-V$ characteristics of the dark current and photocurrent of ZnO nanowire-based devices decorated with and without Au nanoparticles under 350 nm UV-light illumination (with a power density of 20 mW/cm^2) . The $I-V$ characteristics in the dark are nonlinear, indicating that a good Schottky contact was formed between the ZnO nanowire and the Pd microelectrode. The dark currents of the blank-ZnO-based and Au nanoparticle-decorated detectors at 2 V are 85.5 and 335 nA, respectively. Under 350 nm UV-light illumination, the photocurrent of the blank-ZnO-based devices increased by 2 orders of magnitude and that of device with Au nanoparticles increased by 2.89 × 10^6 fold. This is probably because photonic energy (350 nm, 3.54 eV) is higher than the band gap of ZnO (3.4 eV), which can alter the electrical conductivity of ZnO due to the formation of electron−hole pairs. Therefore, the photocurrent results from ZnO nanowires and the Schottky contact. As shown in Figure 5a, the dark current of the device decorated with Au nanoparticles decreased, and the photocurrent increased. After the ZnO nanowire was decorated with Au nanoparticles, abundant small local Schottky contacts were generated on the surface of the ZnO nanowire, i.e., the light response characteristics of Au nanoparticles DEP-assembled detector enhanced significantly.

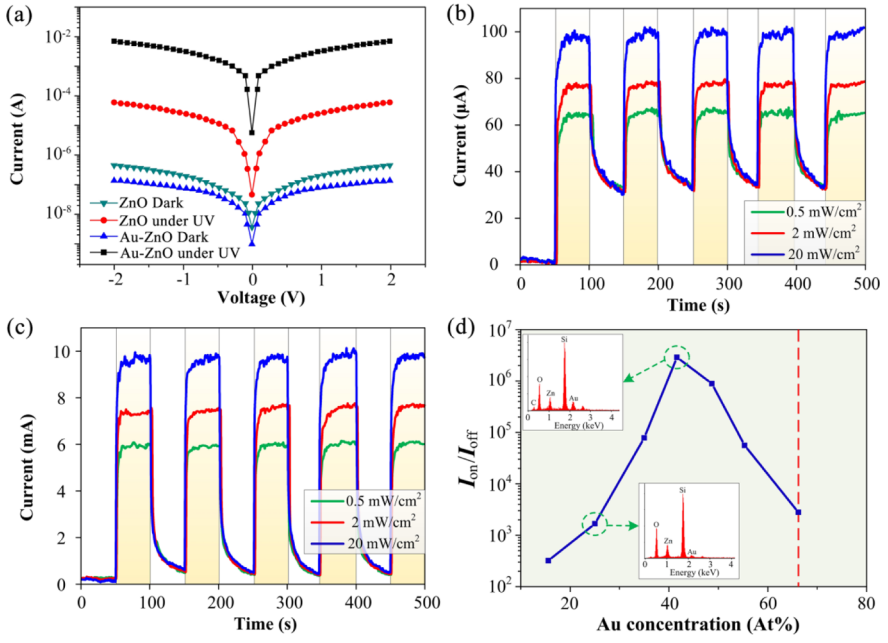

Figure 5. (a) $I-V$ characteristics of the dark current and photocurrent of ZnO nanowire-based devices decorated with and without Au nanoparticles under 350 nm UV-light illumination at 2 V bias. Time-dependent photoresponses of ZnO nanowire-based detectors at 2 V dias without (b) and with (c) Au nanoparticles. (d) Dependence of the ratio of photocurrent to dark current on Au concentration (inset: Au concentration by energy-dispersive X-ray spectroscopy in an Au−ZnO heteronanostructure between the microelectrode pair).

DOI: 10.1021/acsami.5b01362
ACS Appl. Mater. Interfaces 2015, 7, 12713−12718

Figure 5b shows that the photocurrent of the blank-ZnO-based device increases rapidly and reaches saturation quickly under 350 nm UV-light illumination (with power densities of 0.5, 2, and 20 mW/cm^2), while it takes 50 s to reduce to 23% of the maximum current when UV light is turned off (illumination with a power densities of 20 mW/cm^2). In contrast, the current of the device decorated with Au nanoparticles increased more quickly under light illumination and decreased more rapidly when UV light was turned off (Figure 5c). The rise time is defined as the time when the current reaches 63% of the maximum; the rise times of the devices without and with nanoparticles were 0.65 and 0.40 s, respectively. If the decay time is defined as the time when the current decreases to 37% of the maximum, the decay time decreased from 22 to 1.5 s. This indicates that the recovery time of the device with Au nanoparticles decreased significantly.

In the following section, we studied the impact of Au concentration on the ratio of photocurrent to dark current, as shown in Figure 5d. Au concentration in the heteronanostructure between the microelectrode pair was determined by energy-dispersive X-ray spectroscopy. When the frequency of DEP assembly of Au nanoparticles is 1 MHz, the Au concentration is 15.6 atom %. The case of the ratio of photocurrent to dark current increase remained steady and reached a peak 41.6 atom % (f = 500 kHz). Then the ratio fell sharply and reached the lowest point on 66.3 atom % (f = 100 kHz). With the increase of Au concentration over the point, the voltage monitored on the oscilloscope would experience a sharp drop, which means the nanoparticles have patterned a chain and bridged the electrode pair.

The increase in the photocurrent of ZnO nanowires decorated with Au nanoparticles can be explained by the energy spectrum of the nanomaterials. As shown in Figure 6, the surface of the ZnO nanowire is an adsorption site for oxygen molecules, producing free electrons in the dark ($O_2 + e^- \rightarrow O_2^-$). Therefore, the spatial density of carriers can be redistributed, and a space−charge region is formed on the surface. When the device is illuminated by UV light, photogenerated holes move rapidly toward the ZnO surface, thus eliminating the chances to recombine the electron−hole pairs. The gain of photocurrent can be explained by surface-electric-field-induced electron−hole separation effect. The surface band bending and width induced by the charged oxygen molecules increase with density. It is difficult to determine the surface barrier between a ZnO nanowire and an Au nanoparticle, because the charge distribution of Au nanosized particles is different from the classical Schottky model. However, the Schottky contact between a ZnO nanowire and an Au nanoparticle can be determined from the difference between the work functions of Au and ZnO (Au, 5.1 eV; ZnO, 4.3−4.6 eV). The Au nanoparticles on the surface of a ZnO nanowire can be regarded as local Schottky contact points, which can improve the surface band bending. Compared with the blank ZnO-based detector, the electron−hole separation effect is more significant, decreasing the electron lifetime. Therefore, the rest of the photogenerated electrons in the middle of the ZnO nanowire improved the photocurrent.

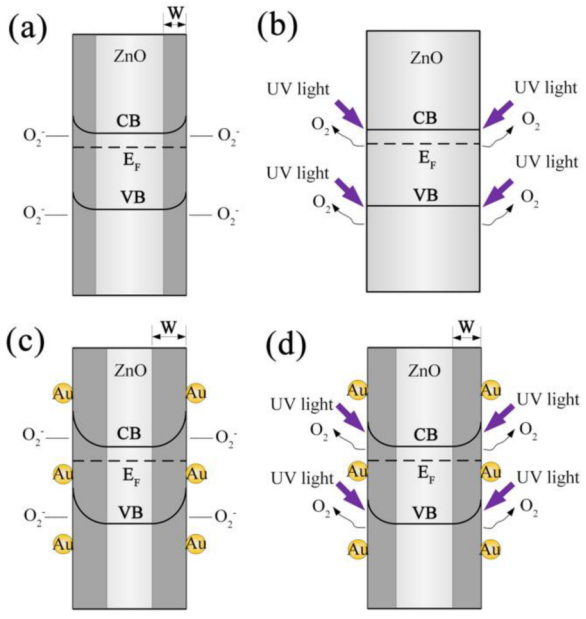

Figure 6. Energy band diagrams for ZnO nanowire-based detectors without (a and b) and with Au nanoparticles (c and d) in the dark (a and c) and under UV illumination (b and d).

4. CONCLUSION

This paper presents a two-step DEP assembly method for fabricating an Au−ZnO heteronanostructure cost efficiently for UV detection. First, DEP assembly of ZnO nanowires dispersed in DI water was studied in a planar microelectrode system. With increasing frequency, the number of DEP-assembled ZnO nanowires decreases apparently under the same DEP assembly time. At 600 kHz, just one ZnO nanowire can be captured between the microelectrode pair, which indicates the ac frequency employed exerts an influence on the DEP assembly behavior of ZnO nanowires. After the DEP assembly of Au nanoparticles under 3 V and 500 kHz, numerous Au nanoparticles aggregated on the surface of the ZnO nanowires and covered the surface. The DEP force on Au nanoparticles was calculated to explain the results of the experiment. The spatial distribution of the particle DEP force around a ZnO nanowire at 3 V and 500 kHz between the electrodes indicates that the forces applied on the nanoparticles in the vicinity of the ZnO nanowire point to the surface of the wire. Nanoparticles were attracted to the surface of the ZnO nanowires because of a stronger field intensity in the region and patterned into a nanoparticle layer to wrap up the ZnO nanowire. Comparative studies were conducted to estimate the photoresponse of the ZnO-based devices with and without Au nanoparticles. After the adsorption of Au nanoparticles, the ratio of photo-to-dark current of the ZnO nanowire-based detector was improved significantly, and the photoresponse was accelerated considerably.

AUTHOR INFORMATION

Corresponding Author

*E-mail: jyshao@mail.xjtu.edu.cn.

Notes

The authors declare no competing financial interest.

ACKNOWLEDGMENTS

This work was mainly supported by the NSFC Major Research Plan on Nanomanufacturing (grant no. 91323303), NSFC

DOI: 10.1021/acsami.5b01362
ACS Appl. Mater. Interfaces 2015, 7, 12713−12718

Fund (Nos.51421004 and 51275401), and Shaanxi Young Talents in Science and Technology (2013KJXX-047).

REFERENCES

(1) Vj, L.; Oh, J.; Nayak, A. P.; Katzenmeyer, A. M.; Gilchrist, K. H.; Grego, S.; Kobayashi, N. P.; Wang, S.; Talin, A. A.; Dhar, N. K.; Islam, M. S. A Perspective on Nanowire Photodetectors: Current Status, Future Challenges, and Opportunities. *IEEE J. Sel. Top. Quantum Electron* **2011**, *17*, 1002−1032.
(2) Zhang, F.; Ding, Y.; Zhang, Y.; Zhang, X.; Wang, Z. L. Piezo-phototronic Effect Enhanced Visible and Ultraviolet Photodetection Using a ZnO−CdS Core−Shell Micro/nanowire. *ACS Nano* **2012**, *6*, 9229−9236.
(3) Ra, H.; Choi, K.; Kim, J.; Hahn, Y.; Im, Y. Fabrication of ZnO Nanowires Using Nanoscale Spacer Lithography for Gas Sensors. *Small* **2008**, *4*, 1105−1109.
(4) Lin, P.; Yan, X. Q.; Zhang, Z.; Shen, Y. W.; Zhao, Y. G.; Bai, Z. M.; Zhang, Y. Self-Powered UV Photosensor Based on PEDOT:PSS/ZnO Micro/Nanowire with Strain-Modulated Photoresponse. *ACS Appl. Mater. Interfaces* **2013**, *5*, 3671−3676.
(5) Liu, S.; Ye, J.; Cao, Y.; Shen, Q.; Liu, Z.; Qi, L.; Guo, X. Tunable Hybrid Photodetectors with Superhigh Responsivity. *Small* **2009**, *5*, 2371−2376.
(6) Guo, L.; Zhang, H.; Zhao, D.; Li, B.; Zhang, Z.; Jiang, M.; Shen, D. High responsivity ZnO nanowires based UV detector fabricated by the dielectrophoresis method. *Sens. Actuators B* **2012**, *166−167*, 12−16.
(7) Kumar, S.; Seo, Y.; Kim, G. Manipulation and trapping of semiconducting ZnO nanoparticles into nanogap electrodes by dielectrophoresis technique. *Appl. Phys. Lett.* **2009**, *94*, 153104.
(8) Ren, S.; Fan, G.; Qu, S.; Wang, Q. Enhanced H2 sensitivity at room temperature of ZnO nanowires functionalized by Pd nanoparticles. *J. Appl. Phys.* **2011**, *110*, 84312.
(9) Pradel, K. C.; Wu, W.; Zhou, Y.; Wen, X.; Ding, Y.; Wang, Z. L. Piezotronic Effect in Solution-Grown p-Type ZnO Nanowires and Films. *Nano Lett.* **2013**, *13*, 2647−2653.
(10) Hu, Y.; Klein, B. D. B.; Su, Y.; Niu, S.; Liu, Y.; Wang, Z. L. Temperature Dependence of the Piezotronic Effect in ZnO Nanowires. *Nano Lett.* **2013**, *13*, 5026−5032.
(11) Wei, Y.; Ding, Y.; Li, C.; Xu, S.; Ryo, J.; Dupuis, R.; Sood, A. K.; Polla, D. L.; Wang, Z. L. Growth of Vertically Aligned ZnO Nanobelt Arrays on GaN Substrate. *J. Phys. Chem. C* **2008**, *112*, 18935−18937.
(12) Hsu, C.; Chang, S. Doped ZnO 1D Nanostructures: Synthesis, Properties, and Photodetector Application. *Small* **2014**, *10*, 4562−4585.
(13) Fan, H. J.; Werner, P.; Zacharias, M. Semiconductor Nanowires: From Self-Organization to Patterned Growth. *Small* **2006**, *2*, 700−717.
(14) Dhara, S.; Giri, P. K. Improved fast photoresponse from Al doped ZnO nanowires network decorated with Au nanoparticles. *Chem. Phys. Lett.* **2012**, *541*, 39−43.
(15) Chen, M. W.; Chen, C. Y.; Lien, D. H.; Ding, Y.; He, J. H. Photoconductive enhancement of single ZnO nanowire through localized Schottky effects. *Opt Express* **2010**, *18*, 14836−14841.
(16) Lin, Y.; Hsueh, Y.; Wang, C.; Wu, J.; Perng, T.; Shih, H. C. Enhancing the Photon-Sensing Properties of ZnO Nanowires by Atomic Layer Deposition of Platinum. *Electrochem. Solid-State Lett.* **2010**, *13*, K93−K95.
(17) Lin, D.; Wu, H.; Zhang, R.; Pan, W. Enhanced Photocatalysis of Electrospun Ag−ZnO Heterostructured Nanofibers. *Chem. Mater.* **2009**, *21*, 3479−3484.
(18) Lin, D.; Wu, H.; Zhang, W.; Li, H.; Pan, W. Enhanced UV photoresponse from heterostructured Ag−ZnO nanowires. *Appl. Phys. Lett.* **2009**, *94*, 172103.
(19) Brewster, M. M.; Zhou, X.; Lim, S. K.; Gradečak, S. Role of Au in the Growth and Nanoscale Optical Properties of ZnO Nanowires. *J. Phys. Chem. Lett.* **2011**, *2*, 586−591.
(20) Hou, X.; Wang, L.; He, G.; Hao, J. Synthesis, optical and electrochemical properties of ZnO nanorod hybrids loaded with high-density gold nanoparticles. *CrystEngComm* **2012**, *14*, 5158−5162.
(21) Hermanson, K. D. Dielectrophoretic Assembly of Electrically Functional Microwires from Nanoparticle Suspensions. *Science* **2001**, *294*, 1082−1086.
(22) Taff, B. M.; Voldman, J. A Scalable Addressable Positive-Dielectrophoretic Cell-Sorting Array. *Anal. Chem.* **2005**, *77*, 7976−7983.
(23) Bhatt, K. H.; Velev, O. D. Control and Modeling of the Dielectrophoretic Assembly of On-Chip Nanoparticle Wires. *Langmuir* **2004**, *20*, 467−476.
(24) Ding, H.; Liu, W.; Shao, J.; Ding, Y.; Zhang, L.; Niu, J. Influence of Induced-Charge Electrokinetic Phenomena on the Dielectrophoretic Assembly of Gold Nanoparticles in a Conductive-Island-Based Microelectrode System. *Langmuir* **2013**, *29*, 12093−12103.
(25) Yang, M.; Zhang, X. Electrical assisted patterning of cardiac myocytes with controlled macroscopic anisotropy using a microfluidic dielectrophoresis chip. *Sens. Actuators A* **2007**, *135*, 73−79.
(26) Ding, H.; Liu, W.; Ding, Y.; Shao, J.; Zhang, L.; Liu, P.; Liu, H. Particle clustering during pearl chain formation in a conductive-island based dielectrophoretic assembly system. *RSC Adv.* **2014**, *5*, 5523−5532.
(27) Gupta, S.; Alargova, R. G.; Kilpatrick, P. K.; Velev, O. D. On-Chip Dielectrophoretic Coassembly of Live Cells and Particles into Responsive Biomaterials. *Langmuir* **2010**, *26*, 3441−3452.
(28) Ding, H.; Shao, J.; Ding, Y.; Liu, W.; Li, X.; Tian, H.; Zhou, Y. Effect of island shape on dielectrophoretic assembly of metal nanoparticle chains in a conductive-island-based microelectrode system. *Appl. Surf. Sci.* **2015**, *330*, 178−184.
(29) Freer, E.; Grachev, O.; Stumbo, D. High-yield self-limiting singlenanowire assembly with dielectrophoresis. *Nat. Nanotechnol.* **2010**, *5*, 525−530.
(30) Kiasari, N. M.; Servati, P. Dielectrophoresis-assembled ZnOnaonwire oxygen sensors. *IEEE Electron Device Lett.* **2011**, *32*, 982−984.
(31) Li, M.; Bhiladvala, R. B.; Morrow, T. J.; Sioss, J. A.; Lew, K.-K.; Redwing, J. M.; Keating, C. D.; Mayer, T. S. Bottom-up assembly of large-area nanowire resonator arrays. *Nat. Nanotechnol.* **2008**, *3*, 88−92.
(32) Kind, H.; Yan, H.; Messer, B.; Law, M.; Yang, P. D. Nanowire Ultraviolet Photodetectors and Optical Switches. *Adv. Mater.* **2002**, *14*, 158−160.
(33) Green, N. G.; Ramos, A.; Morgan, H. Numerical solution of the dielectrophoretic and travelling wave forces for interdigitated electrode arrays using the finite element method. *J. Electrost.* **2002**, *56*, 235−254.
(34) Dimaki, M.; Bøggild, P. Dielectrophoresis of carbon nanotubes using microelectrodes: a numerical study. *Nanotechnology* **2004**, *15*, 1095−1102.
(35) Castellanos, A.; Ramos, A.; González, A.; Green, N. G.; Morgan, H. Electrohydrodynamics and dielectrophoresis in microsystems: scaling laws. *J. Phys. D: Appl. Phys.* **2003**, *36*, 2584−2597.

DOI: 10.1021/acsami.5b01362
ACS Appl. Mater. Interfaces 2015, 7, 12713−12718